# The Effects of Cylindrical Surface Modifications on Turbulent Boundary Layers

J. B. Johansen*
*Raytheon Corporation, Portsmouth, Rhode Island*
and
C. R. Smith†
*Lehigh University, Bethlehem, Pennsylvania*

**A study employing hydrogen bubble wire flow visualization and hot-film anemometry measurements has been conducted to determine the effects of sublayer-scale streamwise surface modifications on the structure and flow characteristics of turbulent boundary layers. The visualization results indicate that the surface modifications did affect the streak spacing characteristics, with the greatest effect occurring for $s^+ < 100$. However, for $y^+ > 10$, the determined streak spacing distributions and statistics appear to relax back to those characteristics of an unmodified surface. Mean velocity and turbulence intensity profiles determined for the modified surfaces indicate essential similarity with those of conventional turbulent boundary layers with variations occurring only near the modified surface. Momentum balances employing the measured velocity profiles indicate that the modifications cause an increase in total surface drag in comparison with an unmodified flat plate. The degree of drag increase shows an apparent correspondence with a narrowing of the line spacing. A hypothesis correlating the increase in drag with changes in the low-speed streak structure by the surface modifications is proposed.**

## Nomenclature

| | |
|---|---|
| $h^+$ | = nondimensional height of modifications, $\equiv hU_\tau/\nu$ |
| $Re_\theta$ | = momentum thickness Reynolds number, $\equiv \theta U/\nu$ |
| $s^+$ | = nondimensional spanwise spacing of modifications, $\equiv sU_\tau/\nu$ |
| $t^+$ | = nondimensional time, $\equiv tU_\tau^2/\nu$ |
| $U$ | = freestream velocity outside boundary layer |
| $u$ | = time-averaged, local streamwise velocity |
| $U_\tau$ | = friction or shear velocity |
| $U^+$ | = nondimensional streamwise velocity, $\equiv u/U_\tau$ |
| $x^+$ | = nondimensional streamwise distance, $\equiv xU_\tau/\nu$ |
| $y^+$ | = nondimensional normal distance to plate, $\equiv yU_\tau/\nu$ |
| $y^+_{\text{wire}}$ | = bubble wire distance above plate, $\equiv y_{\text{wire}}U_\tau/\nu$ |
| $\theta$ | = momentum thickness |
| $\lambda^+$ | = nondimensional streak spacing, $\equiv \lambda U_\tau/\nu$ |

## Introduction

PAST studies of the detailed structure of turbulent boundary layers have shown that the flow structure very near the surface exhibits a pattern of alternating low- and high-speed "streaks,"[1,2] with the periodic breakup of the low-speed streaks (termed "bursting") responsible for almost all of the production of turbulent energy.[3] Capitalizing upon this knowledge of the near-wall flow behavior, several studies have examined the potential for modification of this turbulence structure using passive surface modifications oriented in the streamwise direction.[4-6] Generally, the motivation of these studies has been to develop means for reduction of surface drag by turbulence modification/control. It is suggested that a viable drag reduction mechanism may exist if streamwise surface modifications can force the streak spacing to increase, thus causing burst intensity (bursts per unit area) to decrease. On the other hand, if streak spacing is forced to decrease or burst intensity should increase due to the streamwise surface modifications, surface drag should increase as a result of increased momentum transfer.

Most of the previously examined streamwise surface modifications have all been larger than 10 viscous units—in excess of the height of the viscous sublayer. However, the origin of streaks within the viscous sublayer suggests that the mechanism for their formation, and thus the initiation of the turbulent momentum exchange process, must also develop within or in close proximity to this region. Thus, it is felt that modifications of the order of the viscous sublayer should have a significant effect on the streak formation mechanism, since they will influence the streaks from inception to $y^+ \cong 10$, where the bursting process is initiated.

The present study uses both flow visualization and anemometry measurements to examine the effect of sublayer-scale surface modifications on the qualitative and quantitative characteristics of turbulent boundary layers. Using a specially designed test plate that allows parallel evaluation of modified and unmodified test surfaces under identical flow conditions, specific studies were done to establish the effect of the streamwise modifications on 1) turbulence structure near the wall, 2) conventional turbulence statistics, and 3) surface drag.

## Experimental Facility and Procedure

Experiments were conducted in the Lehigh University free-surface Plexiglass water channel. The working section of the channel is 5 m long, 0.9 m wide, and 0.36 m deep; the water depth for the present studies was maintained at approximately 0.3 m.

The test plate, shown in Fig. 1, is 2.44 m long by 0.895 m wide and is constructed of 6.35 mm Plexiglass with a 6:1 elliptic leading edge. The plate was located 10 cm above the channel floor to eliminate interference from the floor boundary layer. A 3.1 mm diameter rod located 10 cm downstream of the leading edge was used to assure a consistent transition

Received Feb. 12, 1985; presented as Paper 85-0547 at the AIAA Shear Flow Control Conference, Boulder, CO, March 12-14, 1985; revision submitted Nov. 18, 1985. 

*Research Engineer, Submarine Signal Division.

†Professor, Department of Mechanical Engineering and Mechanics.

location. Consistency of the tripped boundary layer was verified by parallel velocity profile measurements at three streamwise locations prior to attachment of the surface modifications.

The modified test surface was created by attaching 0.305 mm monofilament fishing line to an upstream connection plate, stretching the lines over the leading edge, along the top surface, and under the trailing edge, where the lines were attached to a trailing-edge connection plate. By following the contour of the leading edge, abrupt flow obstructions were avoided. The modified portion of the surface was 0.15 m wise, as shown in Fig. 1. This provided the capability to perform parallel studies (either visual or probe) under identical conditions without altering the flow conditions or plate alignment. See Ref. 7 for further details of the flow channel or test plate.

Hydrogen bubble wire visualization employing a 25 $\mu$m diameter platinum wire and bubble-line frequencies of 60 and 120 Hz was generally used. The visualization studies were viewed, recorded, and evaluated using an INSTAR high-speed video system manufactured by the Video Logic Corporation. Employing synchronized strobe lights, the system provides 120 frames/s with an effective shutter speed of 10 $\mu$s (the strobe flash duration). Tapes can be played back in real time, 3-15% real time, slow motion backup, and single-frame sequencing. Hard copy capability is provided by either a videographic printer, which produces single-frame pictures on dry silver paper, or conventional photographs of the video monitor (see Ref. 2 or 8).

Velocity measurements were made using a DISA 55D01 anemometer, DISA 55M25 linearizer, either a single-sensor R11 or R15 hot-film probe, and two TSI 1076 digital voltmeters. To assure stability of mean velocity and turbulence intensity data, all measurements were averaged on the digital voltmeter for 200 s at each measurement location. Data was transferred manually to a DEC VAX 11/780 for the bulk of the analysis. Zero-referencing the probe to the surface was done by adjusting the position of the probe sensor (viewed and magnified by the video system) until the probe sensor support prongs and their image on the reflective wall surface (a 1.5 mm front-surface mirror was used on the surface modifications) appeared to just touch. It was established that this located the center of the sensor 0.2 mm from the surface or the lines.

The probe was calibrated prior to and following each data run. With the channel flow quiescent, the probe was towed through the channel over a range of speeds from zero to approximately 0.35 m/s. The initial set of voltage-velocity data pairs was used to adjust the linearizer prior to profile measurements. During lengthy velocity profile measurements, some tendency for probe drift was noted due to sensor contamination and small temperature changes in the channel ($<\frac{1}{2}$°F due to the use of cooling coils located in the exit tank of the channel). These drift effects were effectively compensated for using the final set of calibration data and a drift rate correction procedure suggested in Ref. 9 and outlined in Ref. 10.

## Experimental Results: Flow Visualization

Both side and plan view hydrogen bubble studies were done. However, appreciable differences in the side view studies were not clearly apparent. In general, the side views suggest that most of the characteristics observed above the line modifications appear essentially the same as those observed above an unmodified flat plate. Thus, the general behavior of turbulent boundary layers in the near-wall region (i.e., bursting behavior) does not appear to be changed by the presence of the modifications; however, it did appear that the modifications, for narrower spanwise spacings, may have created a "focusing" of the location of the bursting over the streamwise lines. This was a subjective evaluation and was not quantified. For comparative pictures and further discussion of the side view behavior, the reader is referred to Ref. 7.

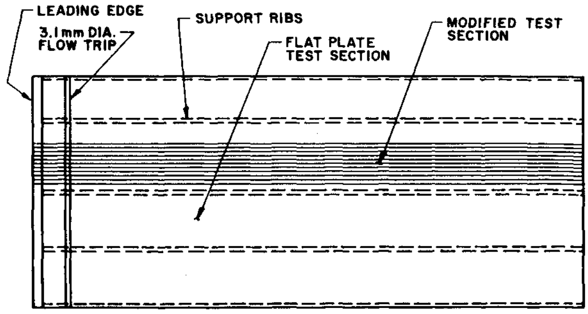


**Fig. 1 Schematic diagram of test plate.**

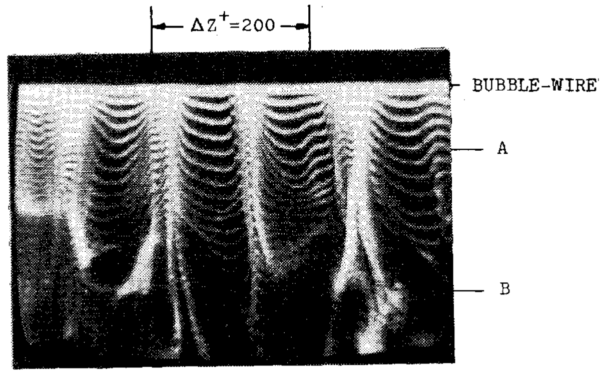


**Fig. 2 Plan view hydrogen bubble line picture showing streaks above the flat plate (flow top to bottom, $Re_\theta \approx 1400$, $y^+_{wire} = 10$).**

Plan view studies were done with the hydrogen bubble wire oriented parallel to the flat plate and perpendicular to the freestream velocity. The wire was attached to the vertical prongs of an overhead, inverted, U-shaped probe that allowed the bubble wire to be positioned at any $y^+$ location above the test surface.

### General Observations: $y^+_{wire} \leq 10$

#### *Flat-Plate Surface*

Figure 2 is a plan view picture of the flow behavior above the unmodified flat plate; note the presence of the characteristic low-speed streak flow structure.[1,2] The bright horizontal line at the top of the picture is the bubble wire; the low-speed streaks appear as the bright streamwise concentrations of bubbles. Note that the streaks are quite straight in the streamwise direction. Lateral movement of the streaks was clearly observed during the study, but the streaks usually remained straight during this movement. The lateral movement of streaks was generally observed when an adjacent streak was bursting, which resulted in pressure fluctuations that affect the location of the adjacent streaks.

Normally, when a streak above a flat plate bursts, most of the streak is ejected downstream and into the outer region of the boundary layer. Generally, streaks do not burst completely. During partial streak bursting, only the downstream portion of the streak appears to be ejected. All fluid upstream of the burst remains as a residual streak, which generally redevelops into a complete streak.

#### *Modified Surface*

Although the flow characteristics above the modified surfaces exhibit some differences from those occurring above a flat plate, the low-speed streaks are still the dominant near-wall flow structure and are essentially the same coherent mechanism in both cases.

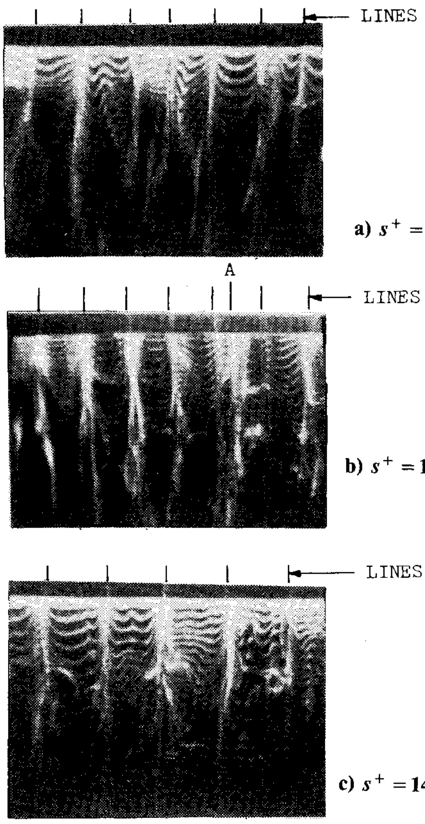


a) $s^+ = 74$, $y^+ = 5$.

b) $s^+ = 111$, $y^+ = 5$.

c) $s^+ = 142$, $y^+ = 10$.

**Fig. 3 Plan view bubble line pictures illustrating good streak to line correlation (flow top to bottom, $Re_\theta \approx 1400$, $h^+ \ngtr 4$).**

Figure 3 is a series of plan view pictures of the streak structure occurring above the modified test section with spanwise line spacing of $s^+ = 71$, 111, and 142, respectively. The monofilament line modifications appear as the light vertical lines upstream of the bubble wire (indicated on the figure). Figure 3 suggests that regardless of $s^+$ the modifications can affect the location and organization of low-speed streaks.

Streaks above modified surfaces were observed to move laterally, but to a lesser degree than those above a flat plate. Streaks forming near a line tended to move toward and focus above that line. The streaks forming above the modified surfaces also tended to behave in a more wavy manner than those forming above a conventional flat plate. As a result of this increased waviness, partial bursting tends to occur more frequently above the modifications than above the flat plate.

### General Observations: $y^+ \geq 10$

The low-speed streaks visualized with $y^+_{\text{wire}} > 10$ do not appear to rigorously coincide with the modifications. The streaks tend to occur farther apart, with apparent streak pairing observed quite frequently. Observations above the modified surface indicate streak behavior very similar to that above a flat plate. Complete streak bursting occurs above both the flat plate and the modifications, but new streaks appear to form more randomly and with less coincidence to the surface modifications than was observed for $y^+_{\text{wire}} \leq 10$. Hence, for $y^+_{\text{wire}} > 10$, the streaks appear to essentially behave the same for both the modifications and the flat plate.

### Streak Spacing

Streak spacing was determined using a series of plan view videographic prints obtained from plan view recordings covering a time duration of $t^+ \cong 10{,}000$. Each print was ob-

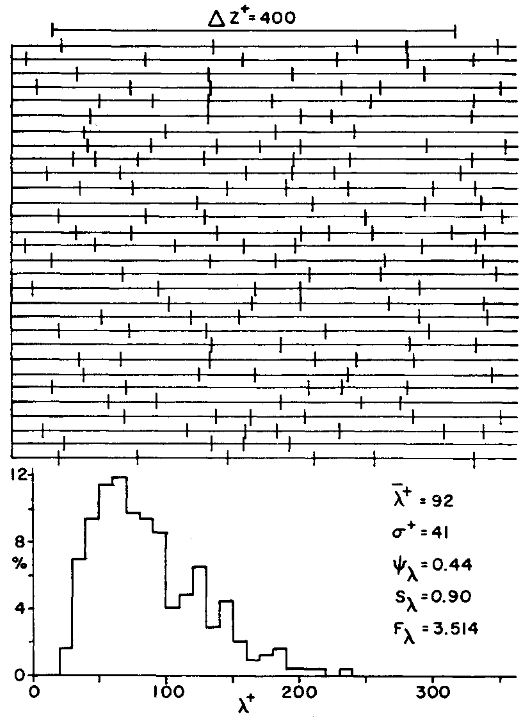


**Fig. 4 Flat-plate streak spacing distribution histogram ($Re_\theta \approx 1400$, $y^+_{\text{wire}} = 5$).**

tained $\Delta t^+ \cong 135$ (100 video frames) apart, roughly of the order of the bursting period for the flow conditions of the present study. This procedure yielded total streak counts between 240 and 700 over the range of conditions examined, yielding a worst case uncertainty of $\pm 5.6\%$ in the mean streak spacing ($\bar{\lambda}^+$) with a 95% confidence level. The streak identification criteria was the same as employed in Ref. 2.

*Histograms*

During the present study, modified surfaces with line heights and spacings of $3.8 < h^+ < 4.5$ and $60 < s^+ < 160$ were examined. Video recordings were made with $y^+_{\text{wire}} = 5$, 10, 15, and 20 above both the modified surfaces and the adjacent flat-plate test section. All studies were conducted at the same $x^+$ location with $Re_\theta \approx 1400$. Spanwise low-speed streak distribution histograms were established from the marked streak count transparencies.

Typical streak spacing distribution histograms are shown in Figs. 4 and 5 (see Ref. 7 for historgrams and corresponding statistics for all streak spacing studies). A reproduction of a part of the streak count transparency used to develop each histogram is shown directly above each histogram. The horizontal lines on the streak counts represent the spanwise axis for each data scene in the sequence, offset in time by $\Delta t^+ = 135$. The vertical lines mark the location of each identified streak. The statistical characteristics of the distribution are listed to the right of each histogram.

A typical flat-plate streak distribution histogram is shown in Fig. 4. Note that the histogram is skewed, with the most probable streak spacing approximately 20% less than the mean, as was observed in Ref. 2. Note that the flatness is only slightly greater than that of a Gaussian distribution ($F = 3.0$), indicating the distribution is slightly peaked.

Figure 5 shows two histograms for a line height of $h^+ = 4$, spanwise spacing of $s^+ = 71$, and $y^+_{\text{wire}} = 5$ and 10, respectively. Note that because of the strongly peaked behavior of the distribution, the scale of the ordinate in Fig. 5a has been compressed relative to the other histograms. Compared to Fig. 4, Fig. 5a demonstrates a radical peak at the mean ($\bar{\lambda}^+ = 71$), which is coincident with the line spacing and

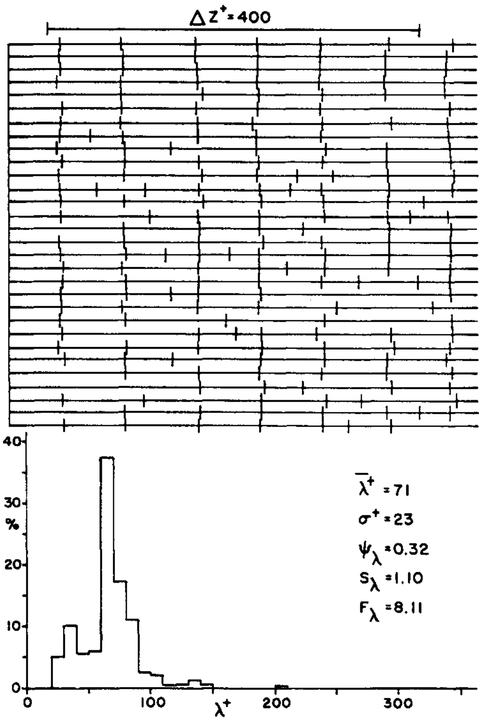


a) $y^+_{\rm wire} \approx 5$.

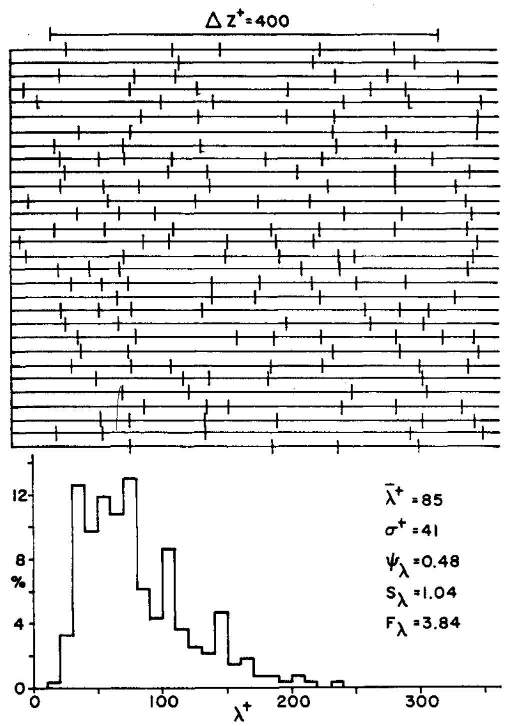


b) $y^+_{\rm wire} \approx 1400$.

**Fig. 5 Modified surface streak spacing distribution histogram ($s^+ = 71$, $h^+ = 4$, $Re_\theta \approx 1400$).**

reflected by a high flatness value ($F_\lambda = 8.11$). The ability of the lines to significantly influence the streak pattern is further demonstrated by the extreme ordering of the streaks in the streak count. Note also that very few streaks occur between lines. The low coefficient of variation ($\psi_\lambda = 0.32$) relative to the comparable flat-plate value of 0.44 further illustrates the stabilizing influence of the lines on the streak pattern. Thus, it appears that very near the wall the lines behave as nucleation sites for streak formation.

a)

b)

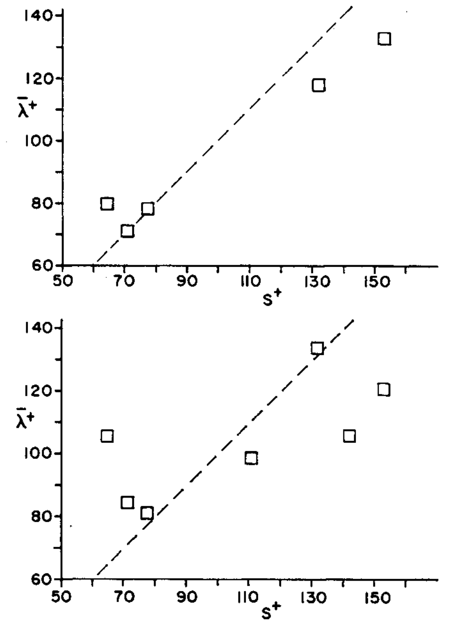


**Fig. 6 Mean streak spacing vs line spacing: a) $y^+_{\rm wire} \approx 5$; b) $y^+_{\rm wire} \approx 10$.**

The streak distribution histogram obtained in Fig. 5b with $y^+_{\rm wire} = 10$ is quite different from that of Fig. 5a. The histogram is no longer peaked and has a much lower flatness value ($F_\lambda = 3.84$). The mean streak spacing is higher than the line spacing, with the streak spacings more widely distributed about the mean ($\bar{\lambda}^+ = 85$), as the coefficient of variation ($\psi_\lambda = 0.48$) confirms. Hence, the distribution approaches that of a flat plate and so too do the associated statistics. The streak count indicates only a slight ordering of the streaks by the lines—significantly less ordering than that observed with $y^+_{\rm wire} = 5$.

Distribution histograms for $s^+ > 71$ suggest that wider spanwise line spacings have a much weaker stabilizing effect on the location of the streaks.[7] For these wider spacings, the lines do appear to create a weak ordering of the streaks; however, the effect is much weaker as the line spacing increases.

*Mean Spanwise Spacing*

The effect of all line spacings on mean streak spacing for all conditions examined is shown in Fig. 6. Note that the dotted line in Fig. 6 is the equivalency line between $\bar{\lambda}^+$ and $s^+$. Figure 6a, determined for $y^+_{\rm wire} \cong 5$, demonstrates a positive relationship between line spacing and mean streak spacing, suggesting that the modifications do have a generally stabilizing and ordering influence on the mean streak spacing. Figure 6b demonstrates that the lines still have a positive effect on observed streak spacing out to $y^+_{\rm wire} \approx 10$; however, the effect is diminished, with a less structured mean streak spacing which appears to have relaxed back toward that for an unmodified flat plate. For $y^+ = 15$ and 20, the streak spacing was essentially that of a flat plate for all $s^+$ values.

## Experimental Results: Anemometry Studies

### Mean Velocity Profiles

Data samples of $65 \pm 5$ points were taken to provide smooth boundary-layer velocity profiles. The mean velocity data were first regression fit to the empirically accepted law-of-the-wall equation, $u/U_\tau = 2.44 \ln y^+ + 4.9$, to estimate the skin-friction coefficient $C_f$ and shear velocity $U_\tau$.

Employing the established $u_\tau$ values, the mean velocity data was normalized on inner variables and plotted in law-of-the-wall form. Plots were constructed for measurements both between two lines and above a line for the modified test section, and above the juxtaposed section of flat plate. To provide further insight, plots of the velocity profiles obtained above a modifying line were established using two different references: 1) with $y^+=0$ referenced to the top of the line (Fig. 7a) and 2) with $y^+=0$ referenced to the plate surface (Fig. 7b). Figure 7a ($s^+=71$, $h^+=4$) might at first suggest the lines have little effect on the characteristic law-of-the-wall profile, since the data above and between modifying lines plot closely to each other and to the flat plate profile. However, Fig. 7b, which references all the velocities relative to the flat plate, shows that the lines do create a low-speed zone that appears to strongly influence the law-of-the-wall plot below $y^+=25$-$30$. Unlike three-dimensional surface roughness, which shifts the entire law-of-the-wall plot down and to the right (see Ref. 11), the law-of-the-wall plots for $y^+>30$ appear to be unchanged by the streamwise surface modifications. Also, if the modifications affected the regions of the boundary layer for $y^+>40$, the empirical flatplate law-of-the-wall equation would not match the data in the linear region of the Clauser cross plots, which was not the case.[7]

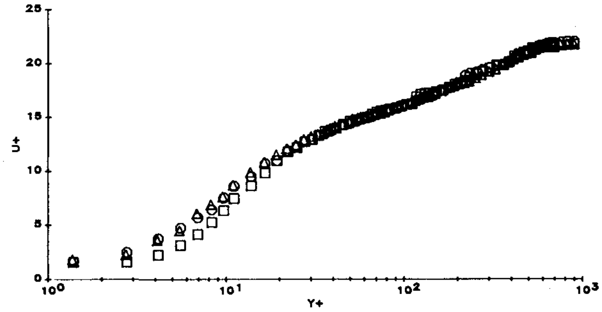

a) Referenced to top of line.

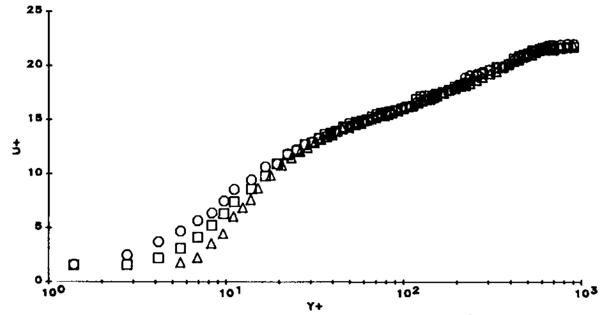

b) Referenced to flat plate.

**Fig. 7 Law-of-wall plot ($s^+=71$, $h^+=4$, $Re_\theta\approx1450$): □ flat plate, ○ between two lines, △ above a line.**

#### Turbulence Intensity Profiles

Turbulence intensity profiles above a modifying line, between two lines, and above the flat plate were measured to determine if the presence of the lines has a damping or amplifying effect on turbulence intensity. Generally, it was found that the lines have little effect on the turbulence intensity profiles.[7] To illustrate this behavior, the wall region data for $y/\delta\leq0.1$ is plotted in Fig. 8. Note that when the data above the line is referenced to the flat plate, this shifts the region of maximum turbulence intensity from $y^+\cong12$ to $\cong17$. Apparently, the presence of the line acts to essentially shift the turbulence behavior by the width of the line. Notice that although there are some small variations in behavior for $y^+\leq10$, any differences have relaxed back to flat plate behavior by $y^+\approx35$, essentially consistent with the previous mean velocity profile results.

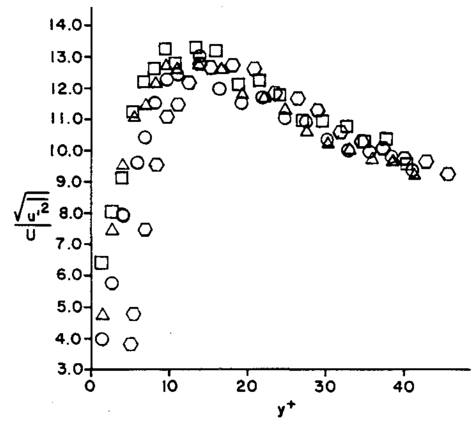

**Fig. 8 Turbulence intensity vs $y^+$ for $y/\delta<0.1$ ($Re_\theta\approx1400$, $s^+=142$, $h^+=4$): □ flat plate, ○ between two lines, △ above a line referenced to top of line, ⬡ above a line referenced to flat plate.**

#### Spanwise Profiles

Figures 9 and 10 illustrate spanwise profiles of mean velocity and turbulence intensity, measured at $y^+=5$ and 10 (referenced to the flat plate) for $s^+=111$ and $h^+=4$. The center of the hot-film sensor was located above a line at the start of the profiles and the probe was traversed in a spanwise direction for two line spaces. As might be expected, Fig. 9 demonstrates the presence of a mean velocity deficit above the lines for both $y^+=5$ and 10, with the deficit diminishing with increasing $y^+$. The actual velocity deficit is probably greater than that indicated in Fig. 9, because the hot-film sensor (which is four times longer than the diameter of the lines) in effect "filters" or averages out sharply varying velocity gradients. Reference 5 also observed the mean velocity to be less above rectangular streamwise modifications than between the modifications. Their study also suggested turbulence intensity to be greater above than between modifications. At $y^+=5$, Fig. 10a suggests that the turbulence intensity is lower above the lines than between them. However, one must keep in mind that the modifications of Ref. 5 extended through the buffer layer and, therefore, were influencing the boundary layer outside the viscous sublayer where the dynamics of the flow are markedly different.

#### Momentum Balance

To establish the degree of drag modification by the modified surface, momentum balances over both the modified surface and the comparable flat plate section were performed. It can be shown that for boundary-layer development with parallel flow over a flat plate with constant freestream velocity, the total surface drag is given by

$$\mathrm{Drag}/\rho U^2=\Delta\theta=\theta_{\mathrm{final}}-\theta_{\mathrm{initial}} \tag{1}$$

indicating that the total surface drag over a region is directly proportional to the change in momentum thickness over the region. Accounting for a slight acceleration of the freestream flow due to boundary-layer blockage effects indicates that Eq. (1) is in error by no more than 1%.

Since the modifications ran the entire length of the test plate, this means that $\theta_{\mathrm{initial}}=0$ for both the modified and flat-plate test sections (at the plate leading edge). Therefore, the drag of the modified surface relative to the flat plate is given by,

$$\mathrm{Drag}/_{\mathrm{mod}}/\mathrm{Drag}_{\mathrm{flat}}=\theta_{\mathrm{mod}}/\theta_{fp} \tag{2}$$

Employing the measured mean velocity profile pairs obtained at $x\cong2$ m for three different $s^+$ values (note: $\theta_{\mathrm{mod}}$ is taken as

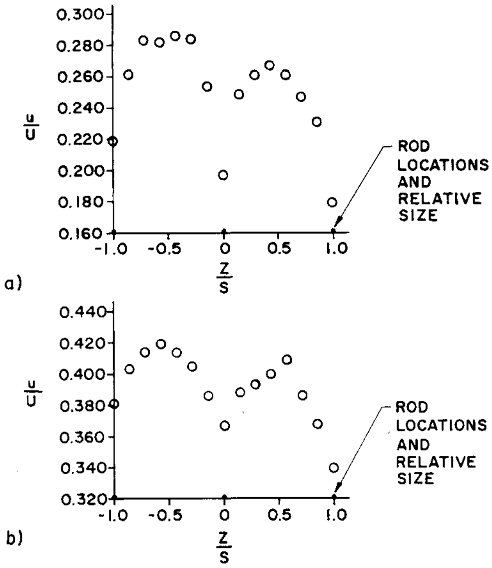


Fig. 9 Transverse mean velocity profiles ($Re_\theta \approx 1500$, $s^+ = 111$, $h^+ = 4$): a) $y^+ = 5$; b) $y^+ = 10$.

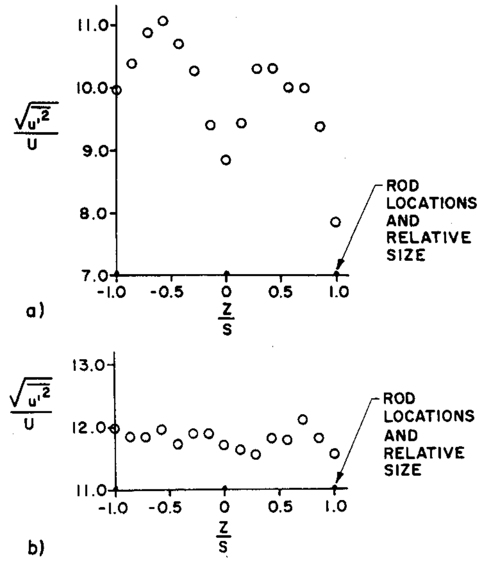


Fig. 10 Transverse turbulence intensity profiles (same conditions as Fig. 9).

the average of above line and between line values), $\theta_{mod}/\theta_{fp}$ ratios were determined via trapezoidal integration and are shown in Fig. 11; although the data are limited, the three points shown suggest that the total friction drag for the modified test sections was always slightly greater than that of the adjacent flat-plate test sections, with $\theta_{mod}/\theta_{fp}$ apparently increasing with decreasing $s^+$. For comparison, $\bar{\lambda}^+$ vs $s^+$ data obtained from the visual studies are also shown in Fig. 11. Since $\bar{\lambda}^+$ is observed to decrease with decreasing $s^+$, this suggests that a decrease in line spacing forces a decreased streak spacing, which in turn increases streak bursting per unit area, yielding an increase in surface momentum exchange which manifests itself as increased surface drag (i.e., an increased $\theta_{mod}/\theta_{fp}$). Thus, the modified surfaces examined here do not appear to have the potential for reducing surface friction drag, but they clearly indicate an apparent relationship between the number of streaks present on a surface and the relative friction drag of that surface.

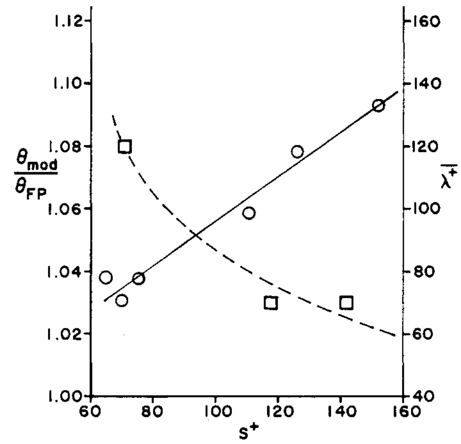

Fig. 11 Mean streak spacing and $\theta_{mod}/\theta_{fp}$ vs line spacing ($Re_\theta = 1300\text{-}1600$): ○ $\bar{\lambda}^+$, □ $\theta_{mod}/\theta_{fp}$.

## General Discussion

The results of the present study indicate that for $y^+ \leq 10$ the statistical characteristics of the spanwise spacing of low-speed streaks can be influenced by the presence of cylindrical streamwise surface modifications that scale on the order of the viscous sublayer. Both the normal and transverse mean velocity profiles indicate the presence of a velocity deficit about the lines for a distance out to about $y^+ \cong 30$. The lines apparently act as an extension of the plate, causing spanwise perturbations in the vorticity sheet at the surface that give rise to spanwise distributed "wakes" which act as nucleation sites for low-speed streak development.

As was suggested by the transverse turbulence intensity profile of Fig. 10, the influence of the lines on streak characteristics quickly diminishes for $y^+ \geq 10$. Since $y^+ \cong 12$ is generally accepted as the region of maximum turbulence intensity within a turbulent boundary layer, the decreasing influence of the modifications for $y^+ \geq 10$ may be a result of the process that spawns the large velocity fluctuations in this region. It is speculated that these intense velocity and vorticity fluctuations are the result of a complicated and intense process of streamwise vortex interaction and coalescence, which causes a rapid agglomeration of the smaller streamwise scales created near the plate surface into larger scales farther removed from the surface. Under such a process, streak spacings and characteristics above the streamwise modifications can rapidly revert to these of a conventional flat-plate flow, as was observed.

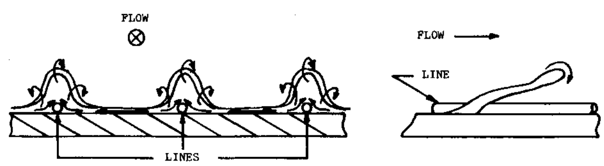


a) End view (looking upstream). b) Corresponding side view.

Fig. 12 Hypothesized hairpin vortex model.

References 8, 12, and 13 have suggested a detailed hairpin or Λ vortex model as an explanation of the origin of low-speed streaks on a flat plate. After observation of 5-6 h of video tape, the present authors propose that a similar hairpin vortex model, with the head of the vortex lying above a line and the vortex legs straddling the line, is a key element in the flow process that causes the low-speed streaks to be influenced by the streamwise surface modifications examined in the present study. Figure 12 is a schematic representation of the speculated hairpin vortex model. The streak formation results from the hairpin vortex legs, which appear as a pair of counter-rotating vortices. These paired vortices interact with low-speed fluid near the surface to pump fluid upward above the line where it combines with the fluid of the line wake to form a low-speed streak region. The counter-rotating vorticity of the adjacent legs of adjacent vortex loops helps to induce the flow of high-speed fluid toward the plate (inflow), where the fluid interacts with the surface (between the surface modifications), is slowed through viscous dissipation, and is subsequently concentrated into the streak above a modification by the pumping action of the paired vortices. Once the streak grows to a minimum size or extent by accretion of fluid, it becomes unstable, breaking down into a new series of hairpin vortices (caused by an inviscid-type instability) that both 1) cause the ejection of low-speed fluid into the outer region (the behavior commonly referred to as a "burst"), and 2) provide the vortex structure for continued reinforcement of the low-speed streaks above the streamwise modifications. This process is consistent with the model of streak formation suggested previously.[8,12,13]

## Conclusions

The effect of streamwise cylindrical surface modifications, of the scale of the viscous sublayer ($h^+ \cong 5$), on the turbulent structure occurring in the near-wall region of turbulent boundary layers was examined using both hydrogen bubble flow visualization and hot-film anemometry measurements. The results of these studies lead to the following conclusions:

1) These types of streamwise surface modifications can influence the low-speed streak formation process near the surface, particularly for spacings of $s^+ < 100$; the apparent effect is to act as a nucleation site causing a focusing of the streak over the modification.

2) The region of influence of these modifications is confined very close to the plate, with the organizing effects of the lines diminishing rapidly after $y^+ \cong 10$.

3) The particular surface modifications examined appear to result in a drag increase compared to identical flat-plate conditions.

4) Reduction of line spacing below the accepted mean streak spacing for a comparable flat-plate flow cause the largest increases in relative drag; the suggested mechanism for this increase is the development of more "bursting" sites due to narrower streak spacing, resulting in elevated surface momentum exchange.

## Acknowledgment

The authors would like to thank the U.S. Air Force Office of Scientific Research for support of this research.

## References

[1]Kline, S. J., Reynolds, W. C., Schraub, F. A., and Runstadler, P. W., "The Structure of Turbulent Boundary Layers," *Journal of Fluid Mechanics*, Vol. 30, Pt. 4, 1967, p. 741.

[2]Smith, C. R., and Metzler, S. P., "The Characteristics of Low-Speed Streaks in the Near-Wall Region of a Turbulent Boundary Layer," *Journal of Fluid Mechanics*, Vol. 129, 1983, p. 27.

[3]Kim, H. T., Kline, S. J., and Reynolds, W. C., "The Production of Turbulence Near a Smooth Wall in a Turbulent Boundary Layer," *Journal of Fluid Mechanics*, Vol. 50, Pt. 1, 1971, p. 133.

[4]Liu, C. K., Kline, S. J., and Johnston, J. P., "An Experimental Study of Turbulent Boundary Layer on Rough Walls," Stanford University, Stanford, CA, Rept. MD-15, 1967.

[5]Nakagawa, H., Nezu, I., and Tominaga, A., "Spanwise Streaky Structure and Macroturbulence in Open-Channel Flows," *Memoirs of the Faculty of Engineering*, Kyoto University, Kyoto, Japan, 1981, p. 34.

[6]Walsh, M. J., "Turbulent Boundary Layer Drag Reduction Using Riblets," AIAA Paper 82-0169, 1982.

[7]Johansen, J. B. and Smith, C. R., "The Effects of Cylindrical Surface Modifications on Turbulent Boundary Layer," Rept. FM-3, Dept. of Mechanical Engineering and Mechanics, Lehigh University, Bethlehem, PA, 1983.

[8]Smith, C. R., "A Synthesized Model of the Near-Wall Behavior in Turbulent Boundary Layers," *Proceedings of Eighth Biennial Symposium on Turbulence*, edited by J. L. Zakin and G. K. Patterson, Dept. of Chemical Engineering, University of Missouri-Rolla, 1984.

[9]Morrow, T. B. and Kline, S. J., "The Performance of Hot-Wire and Hot-Film Anemometers Used in Water," *Flow: Its Measurement and Control*, No. 1, Instrument Society of America, Pittsburgh, PA, 1974.

[10]Bacher, E. V. and Smith, C. R., "An Experimental Study of the Modifying Effects of a Streamwise Grooved Surface of Triangular Cross-Section on the Flow Structure and Statistical Characteristics of Turbulent Boundary Layers," Rept. FM-7, Dept. of Mechanical Engineering and Mechanics, Lehigh University, Bethlehem, PA, 1985.

[11]White, F. M., *Viscous Fluid Flow*, McGraw-Hill Book Co., New York, 1974, p. 440.

[12]Perry, A. E. and Chong, M. S., "On the Mechanism of Wall Turbulence," *Journal of Fluid Mechanics*, Vol. 119, 1982, p. 173.

[13]Acarlar, M. S. and Smith, C. R., "An Experimental Study of Hairpin-Type Vortices as a Potential Flow Structure of Turbulent Boundary Layers," Rept. FM-5, Dept. of Mechanical Engineering and Mechancis, Lehigh University, Bethlehem, PA, 1984.